Hindawi Publishing Corporation
Journal of Nanomaterials
Volume 2013, Article ID 768628, 9 pages
http://dx.doi.org/10.1155/2013/768628

Research Article

Preparation and Biological Properties of Platinum(II) Complex-Loaded Copolymer PLA-TPGS

Ha Phuong Thu,[1] Phan Thi Hong Tuyet,[2] Mai Thi Thu Trang,[1] Nguyen Hoai Nam,[1] Truong Thi Nhu Hieu,[1] Le Quang Duong,[1] Tran Thi Nhu Hang,[3] Tran Thi Hong Ha,[3] Do Huu Nghi,[3] Le Huu Cuong,[3] and Le Mai Huong[3]

[1] *Institute of Materials Science, Hanoi 844, Vietnam*
[2] *Vinh University, Vinh 8438, Vietnam*
[3] *Institute of Natural Products Chemistry, Hanoi 844, Vietnam*

Correspondence should be addressed to Le Mai Huong; lehuong@inpc.vast.vn

Received 1 August 2013; Revised 20 October 2013; Accepted 20 October 2013

Academic Editor: Abdelwahab Omri

A new nanodrug system containing bis(menthone thiosemicarbazonato) Platinum(II) complex (Pt-thiomen) encapsulated with the block copolymers polylactide-d-α-tocopheryl polyethylene glycol 1000 succinate (PLA-TPGS) was prepared by a modified solvent extraction/evaporation technique. The characteristics of the nanoparticles including surface morphology, size distribution, structure, and biological activities such as antimicrobial and cytotoxic activities were *in vitro* investigated. The spherical nanoparticles were around 50 nm in size with core-shell structure and narrow-size distribution. The encapsulated Pt-thiomen can avoid interaction with proteins in the blood plasma. The inhibitory activity of Pt-thiomen-loaded PLA-TPGS nanoparticles on the growth of some bacteria, fungi, and Hep-G2 cells suggests a possibility of developing PLA-TPGS-Pt-thiomen nanoparticles as one of the potential chemotherapeutic agents.

1. Introduction

Platinum(II) complexes, one of the most potent anticancer drugs, have been used for treatment against a variety of human cancers [1, 2]. They are effective cytotoxic agents in the treatment of epithelial malignancies such as lung, head and neck, ovarian, bladder, and testicular cancer [3]. However, their clinical applications is restricted because almost all platinum in the blood plasma are often bound by protein after intravenous injection [4]. The binding of Pt(II) complexes with proteins reduces the urinary excretion of platinum and causes the deposition of Platinum in tissues [5]. The action with proteins causes many side effects including renal and auditory toxicity, nausea, and vomiting [6–8]. The development of drug delivery systems in the last several decades has provided a variety of methods including the incorporation of drugs into liposomes, lipid emulsions, and polymeric micelles to reduce adverse effects, to increase their solubility, and to prolong circulation time as well [9–12]. More recently, a promising approach which has attracted much attention of researchers is the encapsulation of platinum-based anticancer drugs in sterically stabilized polymeric micelles. This strategy has succeeded in reducing toxicity and improving efficacy of encapsulated platinum complex due to an excellent stability in plasma and a much longer circulation time as compared to free Pt(II) complexes [13–16]. The *in vitro* test on antimicrobial activity of the series of platinum(II) complexes by the macrodilution method was also reported by Utku et al. [17]. Some synthesized complexes might be taken into consideration as promising antifungal compounds [18].

To the best of our knowledge, there were a few reports on encapsulation of Pt(II) complex due to the fact that it is an ionic compound and it lacks reactive groups in its molecule (amino, carboxyl, hydroxyl groups for instance). Our previous study on synthesis of complex of Cu(II) with methone thiosemicarbazon revealed that the new complex displayed cytotoxic activity against Hep-G2 and LU (Lung) cell lines (data not shown). In this study, we synthesized a new

Pt(II) complex (Pt-thiomen), fabricated a nanodrug system by incorporating Pt(II) in biodegradable core-shell PLA-TPGS copolymer, and tested the *in vitro* efficacy on cancer cells. Excellent biocompatibility of polylactide (PLA) leads to the US FDA's approval and acceptance (Food and Drug Administration) for medical applications. However, disadvantages of this polymer are high hydrophobicity and slow degradation which make it very difficult to encapsulate drugs. To overcome these hindrances, the hydrophobic blocks as the core are linked with hydrophilic polymers like TPGS as the shell. Thanks to its good biocompatibility, hydrophilicity, and the absence of antigenicity and immunogenicity, the core-shell structure with PLA-TPGS as an outer shell enables the nanoparticles to escape from the scavenging of the reticuloendothelial systems (RES) *in vivo* effectively [12].

2. Materials and Methods

2.1. Materials. Menthone thiosemicarbazone (Hthiomen), Potassium tetrachloroplatinate(II), polylactide (PLA), and d-α-tocophenyl polyethylene glycol 1000 succinate (TPGS) were purchased from Sigma Aldrich (Germany).

2.2. Methods

2.2.1. Synthesis of Pt(II) Complex (Pt-Thiomen). Pt(II) complex (Pt-thiomen) was synthesized from Menthone thiosemicarbazone (Hthiomen) ligand and Potassium tetrachloroplatinate(II) ($K_2[PtCl_4]$). Firstly, Hthiomen was prepared from thiosemicarbazide and (±) menthone (1 : 1 molar ratio). The mixture was dissolved in warm ethanol and anhydrous acetic acid was added until pH reached 3-4 and this was followed by stirring for 3 h. After cooling to room temperature, crystalline product was isolated and washed with water, ethanol, and dried over P_2O_5. Hthiomen was obtained as a white powder. To synthesize Pt-thiomen, a solution of $K_2[PtCl_4]$ (0.415 g, 0.001 mol) in 15 mL water was added to a solution of menthone thiosemicarbazone (0.454 g, 0.002 mol) in 50 mL ethanol at 30°C under stirring for 1 h. The reaction mixture was kept at 0°C for 12 h. Afterwards, the precipitate was filtered off and washed several times with water, ethanol, and dried over P_2O_5. The Pt-thiomen was obtained as a dark yellow powder.

2.2.2. Synthesis of PLA-TPGS Copolymer. PLA-TPGS copolymer was synthesized through ring opening polymerization of poly lactide and d-α-tocopheryl polyethylene glycol 1000 succinate (TPGS) [12]. Briefly, PLA and TPGS with weight ratio of 1 : 4 were dissolved in toluene and added to an ampoule. Stannous octoate was used as catalyst agent. The mixture was vigorously stirred for 10 h at 130°C under nitrogen flow. After polymerization, organic solvent was evaporated overnight and final product was obtained by precipitating in cold methanol and subsequently dried at 60°C for 24 h in inert condition.

Afterwards, 20 mg of copolymer PLA-TPGS was dissolved in dichloromethane and sonicated for 15 min before added to 20 mL of distilled water. The mixture was then stirred at room temperature to get an aqueous solution of PLA-TPGS. The final solution was obtained by centrifugation at 4000 rpm for 5 min to remove any aggregate. The remaining organic solvent in PLA-TPGS solution was evaporated and the product was kept at room temperature for further preparation.

2.2.3. Preparation of PLA-TPGS Loaded Pt-Thiomen Nanoparticles. PLA-TPGS loaded Pt-thiomen nanoparticles were prepared using a modified solvent extraction/evaporation method. Firstly, Pt-thiomen was dissolved in ethanol by sonicating for 15 min with concentration of 0.5 mg mL^{-1}. The solution was then dropped wisely into an aqueous solution of PLA-TPGS nanoparticles (1 mg mL^{-1}) under stirring continuously at room temperature for at least 24 h. Then, the emulsion was gently stirred until the organic solvent was completely evaporated. The unloaded Pt-thiomen was removed by centrifugation at 4000 rpm for 5 min and the soluble product was stored at room temperature.

2.2.4. The Cytotoxicity Assay. The cytotoxicity assay was performed based on the method of Vichai and Kirtikara [19] and Skehan et al. [20] using sulforhodamine B(SRB). In brief, the Hep-G2 cells were cultured in 10% FBS-MEM medium and incubated in 5% CO_2 and 95% air at 37°C for 3 days. The fresh cells were treated with trypsin at 37°C for 5 min and were resuspended in a fresh medium containing 10% FBS to a density of 1×10^4 cells/mL. For activity assay, in triplicate 96-well plates 190 μL of the cell suspension was added in each well which contained 10 μL of test samples with various known concentratiosn prepared in 5% DMSO. Ellipticine was used as the positive reference. The cultured plates were then incubated for 3 days and cells were fixed with 100 μL of 30% trichloroacetic acid for 30 min at 4°C. Unbound protein was removed gently under tap water and the plates were stained for 30 min with 200 μL of 0.4% (w/v) sulforhodamine B (SRB) in 1% acetic acid. Unbound dye was removed by four washes with 200 μL of 1% acetic acid. The stained bound protein was then dissolved in 200 μL of 10 mM unbuffered Tris base(tris (hydroxymethyl)aminomethane) and the optical density was measured in a computer-interfaced, 96-well microplate reader at A540 nm. The SRB assay results were linear with the number of cells and with values for cellular protein measured at densities ranging from sparse subconfluence to multilayered supraconfluence. The signal-to-noise ratio at 515–564 nm was approximately 1.5 with 1,000 cells per well.

2.2.5. Antimicrobial Activity Assay. Antimicrobial activity of test samples was assayed using microbroth dilution methods of Mishra and Kaushik [21] and Vichai and Kirtikara [19]. In brief, the serial dilution technique was performed using 96-well microplates to determine the minimum inhibitory concentration (MIC) of the drugs against test microorganisms.

Gram negative bacteria including *Escherichia coli* (ATCC 25922) and *Pseudomonas aeruginosa* (ATCC 25923) and Gram positive bacteria including *Bacillus subtilis* (ATCC 27212) and *Staphylococcus aureus* (ATCC12222) strains were

used for this assay. To test inhibitory activity of samples on fungi, the filamentous fungi including *Aspergillus niger* (439) and *Fusarium oxysporum* (M42) and yeast including *Candida albicans* (ATCC 7754) and *Saccharomyces cerevisiae* (SH 20) were used. Briefly, the fresh microorganisms were diluted with the growth medium broth to a final inoculum size of 10^5 CFU/mL. The test samples including Pt-thiomen, PLA-TPGS, and PLA-TPGS loaded Pt-thiomen were dissolved in 5% DMSO at various concentrations and then were loaded into 96-well microplates. 190 μL of the culture suspension was loaded onto wells which already contained 10 μL of the test sample with a known concentration. The plates were covered and incubated overnight at 37°C for bacteria and at 30°C for 48 h for fungi. Microbial growth in the well was evaluated by naked eyes and a complete inhibition refers to a clear well. Penicillin, streptomycin, and nystatin were used as positive reference for Gram negative bacteria, Gram positive bacteria, and fungi, respectively. A blank sample was treated in the same way using 5% DMSO instead of the test samples.

2.2.6. Structure Determination. Mass spectroscopy with electrospray ionization technique (ESI-MS) was used in order to confirm the formula of Hthiomen and Pt-thiomen (Agilent 1100 LC/MSD).

IR spectra were recorded with a FTIR Shimadu spectrophometer using KBr discs in the frequency range of 4000–400 cm^{-1}.

^{1}H-NMR spectra were obtained with a Bruker 500 MHz spectrometer and the chemical ship is given in units of δ relative to TMS as an internal using DMSO-d6 as the solvent.

Field emission scanning electron microscope (FE-SEM) images were taken by a Hitachi S-4800. The micelle loaded Pt-thiomen was examined by absorption on a VARIAN spectrophometer Cary 5000 UV-VIS-NIR.

The encapsulation efficiency (EE, %) of Pt-thiomen in micelle was calculated by the following formulation:

$$\begin{aligned}\text{EE}\,(\%) = {} & (\text{total amount of Pt-thiomen} \\ & - \text{nonencapsulated amount of Pt-thiomen}) \\ & \times (\text{total amount of Pt-thiomen})^{-1}.\end{aligned} \tag{1}$$

The nonencapsulated Pt-thiomen was recovered by centrifugation at 4000 rpm for 5 m and the Pt-thiomen as aggregate form was dried and weighed.

3. Results and Discussion

Mass spectroscopy with electron ionization mass spectrometer (EIMS) technique was used in order to confirm the complexes' formula of Pt-thiomen and the results were displayed in MS data (see Table 1). As seen in the MS spectrum (Figure 1(b)), the appearance of a cluster of peaks with m/z = 228, 229, 230 of ligand and a cluster of peaks with m/z = 648, 649, 650, 651 in the spectrum of Pt-thiomen were consistent with the molecular weight of the complexe calculated from different isotopes (Figure 2(b)).

Table 1: MS data and compound's molecular formula.

Number	Sample	m/z, $[M + H]^+$	M	Molecular formula
1	Hthiomen	228	227	$C_{11}H_{21}N_3S$
2	Pt-thiomen	649	648	$PtC_{22}H_{40}N_6S_2$

The ^{1}H-NMR spectrum of Hthiomen (Figure 2(a)) exhibited a singlet at 10.22 ppm attributed to NH-hydrazine proton. The presence of NH signal indicated the presence of Hthiomen in the thione form. The proton signal on the CH=N appeared at 7.40 ppm. It is interesting to notice the presence of two broad single signals for the NH_2-protons, respectively, at 8.00 and 7.21 ppm due to restricted rotation around the C–N bond because of its partial double bond character. The triplet at 0.85 ppm was assigned to 3H of CH_3 group and signals in range 1.61 to 3.13 ppm were assigned to other fourteen protons.

The absence of the H signal (NHC=S group) from Pt-thiomen complex's spectrum (Figure 2(b)) confirmed the deprotonation of the ligand due to coordination with Pt(II) via S and N. The signals of other protons appeared in similar range in ligand's spectra. The NMR results were consistent with IR results.

The IR spectrum of Hthiomen (Figure 3(a)) showed absorption bands at 3433 and 3210 cm^{-1} due to stretching frequencies for NH-amide, while the absorption band for NH-hydrazine is present at 3146 cm^{-1}. The band due to the –SH group was not observed in 2500–2600 cm^{-1} and the presence of band at 823 cm^{-1} due to ν(C=S) suggested the existence of thiosemicarbazone in the thione form. Typical bands for aliphatic –CH appeared in the frequency range 3031–2852 cm^{-1} and the absorption for –CN appeared at 1590 cm^{-1}.

The IR spectrum of Pt-thiomen (Figure 3(b)) showed absorption bands in the region 3200–3400 cm^{-1} due to stretching frequencies for NH-amide, while the absorption for NH at region 3000–3200 cm^{-1} was absent. The ν(C=S) band at 823 cm^{-1} in the spectrum of the ligand shifted to 741 cm^{-1} in the spectrum of the complex Indicating that the existence of ligand is in the thiol form and deprotonation on complexation and that Pt coordinated with the thiolate sulphur. The ν(C=N) band of the thiosemicarbazone at 1590 cm^{-1} shifted to 1600 cm^{-1} in the spectrum of the complexes, indicating coordination of the azomethine nitrogen. This result was confirmed by the presence of new bands at 615 and 472 cm^{-1} due to ν(Pt–N) and ν(Pt–S). These spectra suggest that after deprotonation the ligand coordinated with the Pt(II) via S and N. Selected IR bands for the ligand Hthiomen and complex (Pt-thiomen) are given in IR data (see Table 2).

On the basis of the above analysis, reasonable structures of ligand and Pt-thiomen are depicted in Figure 4.

The FT-IR spectra of PLA-TPGS, Pt-thiomen, and PLA-TPGS-Pt-thiomen were also recorded and presented in Figure 5. The encapsulation efficiency was determined with EE value of 80%. After encapsulated by copolymer PLA-TPGS, the stretching and absorption bands of NH-amide and

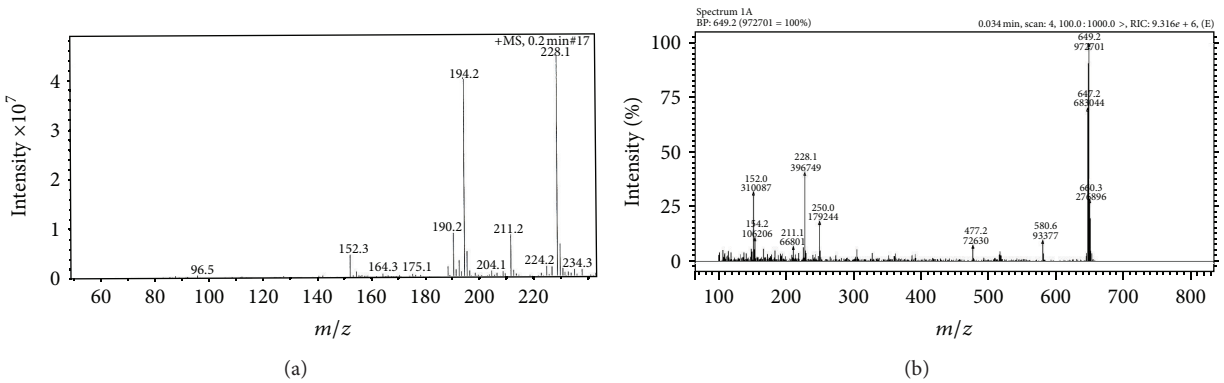

(a) (b)

Figure 1: Mass spectra of Hthiomen (a) and Pt-thiomen (b).

Table 2: Selected IR bands of the Hthiomen and Pt-thiomen.

Number	Compound	ν, cm^{-1}				
		ν_{NH}	ν_{CN}	ν_{NN}	ν_{CS}	$\nu_{Pt\text{-}X}$, $(X = S, N)$
1	Hthiomen	3433, 3210, 3146	1590	1081	823	—
2	Pt-thiomen	3427, 3291	1600	1115	741	615, 472

NH-hydrazine appeared at 3300–3600 and 2900–3100 cm^{-1}, respectively. The peak at 811 cm^{-1} was assigned to oscillation of C=S group while the one at 1623 cm^{-1} was assigned to oscillation of C=N group in Pt-thiomen encapsulated by PLA-TPGS. The absorption band of ν(Pt–N) and ν(Pt–S) shifted to 636 and 482 cm^{-1} after it was encapsulated by the copolymer, respectively. The CH stretching band of PLA-TPGS was observed at 2939 cm^{-1} while the absorption band of hydroxyl group appeared at 3441 cm^{-1}. The appearance of characteristic peaks of Pt-thiomen and PLA-TPGS accompanied by the shift of these peaks confirmed the encapsulation of Pt complexes by synthesized copolymer PLA-TPGS.

Surface morphology of the synthesized nanoparticles is shown in Figures 6(c) and 6(d). FE-SEM images indicated that the PLA-TPGS copolymer (Figures 6(a) and 6(b)) had a round shape with the average diameter of 50 nm. After encapsulating Pt-thiomen, the shape and size of PLA-TPGS-Pt-thiomen nanoparticles did not change much, still in the range of 50 nm (Figures 6(c) and 6(d)). The small size with core-shell structure enables this new nanodrug system to avoid protein binding and to lengthen circulation time in the body thus enhancing the potential to be applied as a chemotherapeutic agent.

PLA-TPGS-Pt-thiomen was tested for the cytotoxic activity in order to evaluate inhibition on Hep-G2 cells. The results show remarkably varying cytotoxic activities of test samples including Pt-thiomen, PLA-TPGS, and PLA-TPGS loaded Pt-thiomen. It was observed that increasing concentration of PLA-TPGS-Pt-thiomen causes a decrease in the cell viability (indicated by % cell survival) (see Table 3). It is clear that the encapsulated Pt-thiomen displayed a higher activity as compared to the free Pt-thiomen (see Figure 7 and Table 3).

Table 3: The cytotoxic activity of PLA-TPGS-Pt-thiomen on Hep-G2 cells.

Number	Concentration (μg/mL)	Cell line Hep-G2	
		Survival (%)	IC_{50} (μg/mL)
1	Ellipticine (reference)	0.32 ± 0.04	0.27
2	Pt-thiomen		
	20	25 ± 0.9	13.6
	10	38 ± 0.2	
	5	80 ± 0.1	
	2.5	91 ± 0.5	
3	PLA-TPGS		
	100	90 ± 0.7	ND
4	PLA-TPGS-Pt-thiomen		
	20	6.8 ± 0.7	5.05
	10	20.6 ± 0.3	
	5	42.5 ± 0.9	
	2.5	73.8 ± 1.1	
	1.25	91.3 ± 0.8	

ND: not detectable.

The images of Hep-G2 cell (presented in Figure 7) indicate that cells were changed in accordance with increasing concentration of PLA-TPGS-Pt-thiome. This new nanoparticle had no activity at the concentration of 1 μg mL^{-1}. At higher concentration ranging from 2.5 to 5 μg mL^{-1} the cell growth and angiogenesis were inhibited and cells were much destroyed at 10 μg mL^{-1} and 20 μg mL^{-1}. In this case, PLA-TPGS-Pt-thiomen may cause necrosis and cell death at high doses.

Antimicrobial activity of PLA-TPGS-Pt-thiomen complex showed a significant activity as compared to that of the starting materials including nonencapsulated Pt-thiomen and PLA-TPGS (see Table 4). In comparison to several standard drugs assayed by other groups [17, 18], the antimicrobial activity of the encapsulated Pt-thiomen was lower, possibly due to its high molecular weight of the polymer. The MIC values of this polymer are found to be 40–80 μg mL^{-1} (see Table 4).

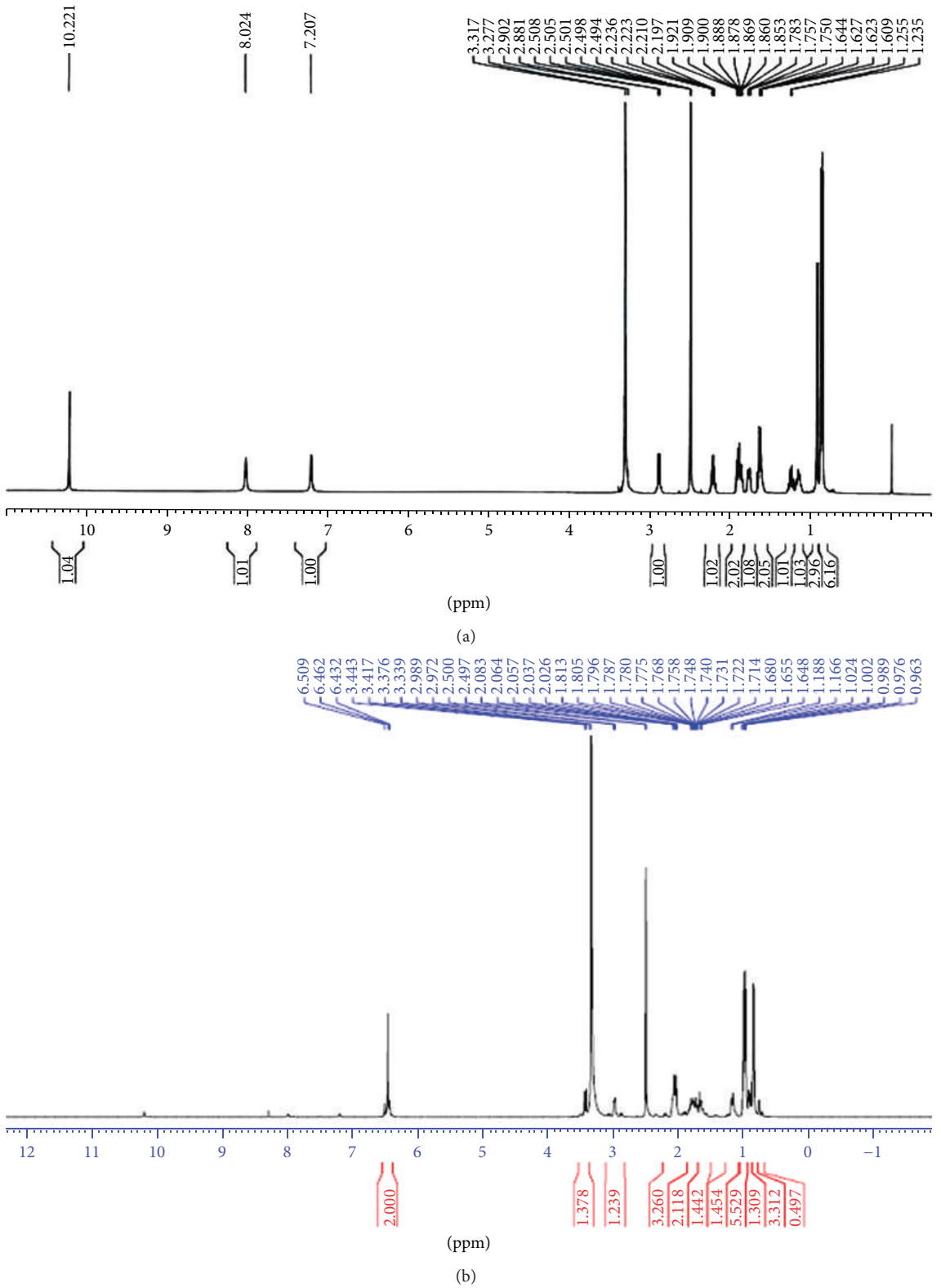

Figure 2: ^{1}H-NMR spectra of Hthiomen (a) and Pt-thiomen (b).

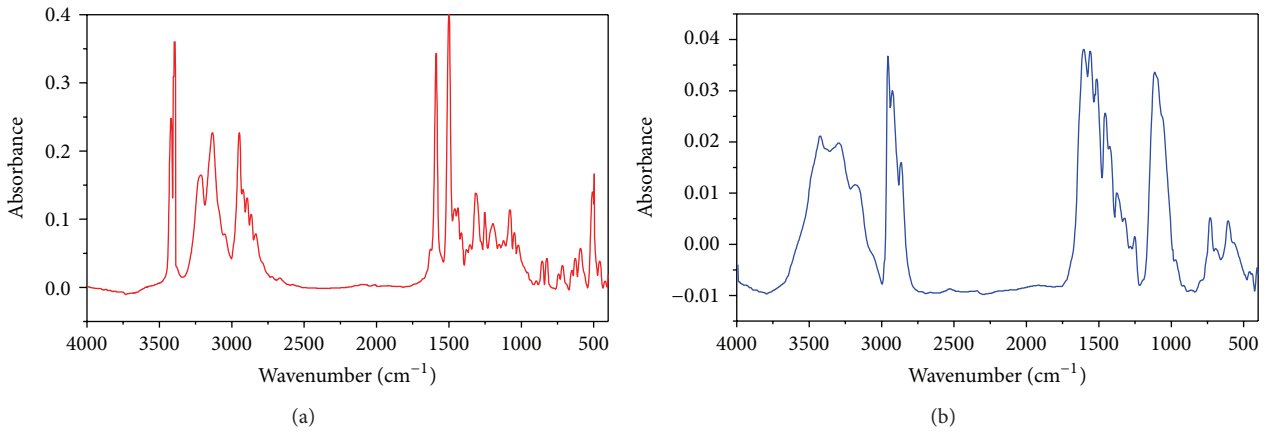

Figure 3: FT-IR spectra of Hthiomen (a) and Pt-thiomen (b).

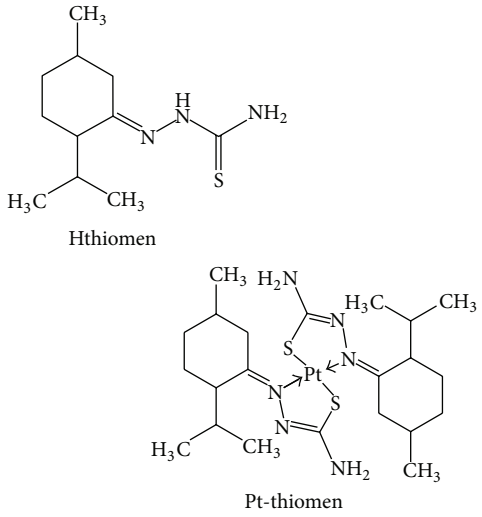

Figure 4: Structures of the Hthiomen and Pt-thiomen.

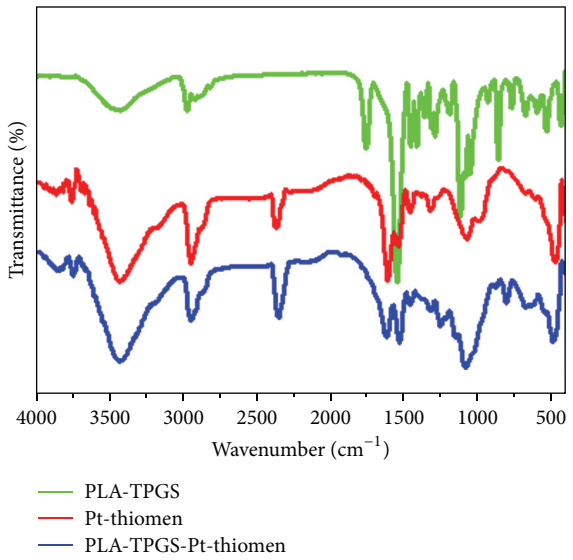

Figure 5: FT-IR spectra of PLA-TPGS, Pt-thiomen, and PLA-TPGS-Pt-thiomen.

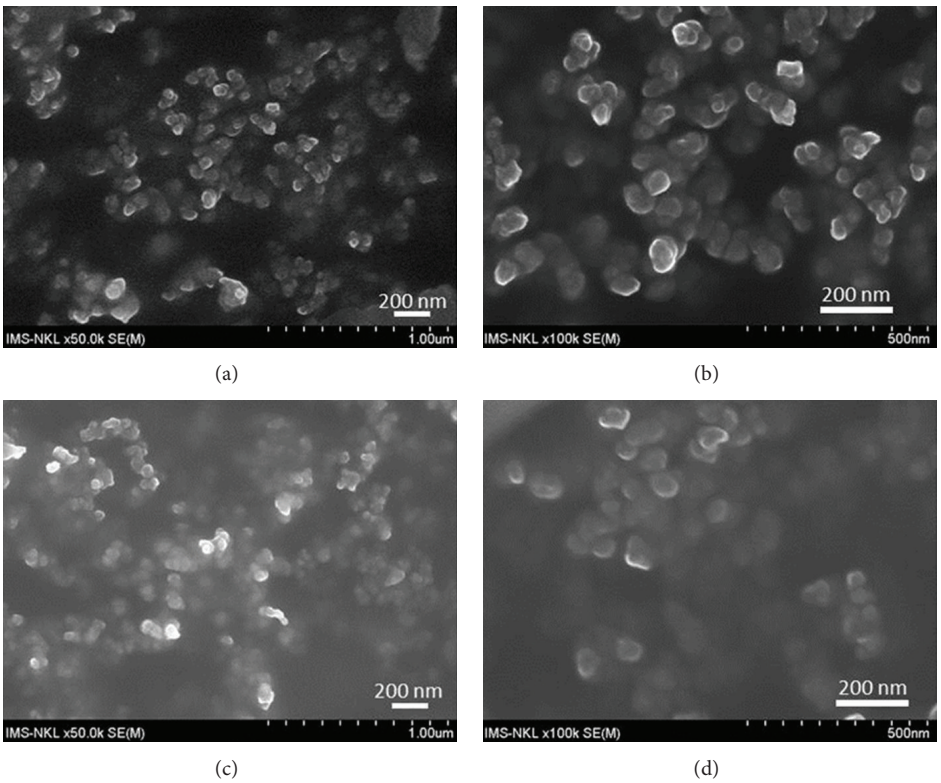

Figure 6: FE-SEM images of PLA-TPGS ((a), (b)) and PLA-TPGS-Pt-thiomen ((c), (d)).

4. Conclusion

In conclusion, PLA-TPGS-Pt-thiomen nanoparticles were successfully synthesized by a modified solvent extraction/evaporation technique. These particles displayed a better solubility in water as compared to unloaded Pt-thiomen. Spherical core-shell structure with the average size of 50 nm may help them avoid protein binding in the blood plasma which often occurs. They seem to be suitable for drug delivery applications. The results of antimicrobial activity of copolymer PLA-TPGS loaded Pt-thiomen nanoparticles show that these nanoparticles were inhibitory to both Gram negative and positive bacteria and fungi including *A. niger* and *S. cerevisiae* but not inhibitory to *F. oxysporum* and *C. albicans*. PLA-TPGS-Pt-thiomen nanoparticles also show a cytotoxic activity on Hep-G2 cells with concentration ranging from 2.5 μg mL^{-1} to 20 μg mL^{-1} and the IC_{50} value of PLA-TPGS-Pt-thiomen is 5.5 μg mL^{-1}.

The finding of bioactivity of the new synthesized complex against Hep-G2 cells and test microorganisms demonstrated the better protection and delivery capacity of PLA-TPGS upon encapsulation of Pt-thiomen. Mechanism remains unclear. Involvement of cell membrane and cytosolic response to this new complex need to be further studied in order to get insight into this observation.

All these results demonstrated a successful design of a new nanodrug system based on Platinum(II) complex (Pt-thiomen) and exhibited a potential application of this system in drug delivery.

Table 4: The MIC values of PLA-TPGS-Pt-thiomen in antimicrobial assay.

Number	Sample	MIC value (μg/mL)							
		E	P	B	S	A	F	S	C
2	Penicillin	5.2	20.8						
3	Streptomycin			7.2	14.4				
4	Nystatin					5.78	2.89	1.445	2.89
5	Pt-thiomen	(—)	(—)	(—)	(—)	(—)	(—)	(—)	(—)
6	PLA-TPGS	(—)	(—)	(—)	(—)	(—)	(—)	(—)	(—)
7	PLA-TPGS-Pt-thiomen	40	80	80	80	40	(—)	80	(—)

(—): no inhibition.
E: *Escherichia coli*; P: *Pseudomonas aeruginosa*; B: *Bacilus subtillis*; S: *Staphylococcus aureus*; A: *Aspergillus niger*; F: *Fusarium oxysporum*; S: *Saccharomyces cerevisiae*; C: *Candida albicans*.

Authors' Contribution

Le Mai Huong and Ha Phuong Thu contributed equally to this work.

Acknowledgments

This work was financially supported by the National Foundation for Science and Technology Development of Vietnam (NAFOSTED) under Grant no. 106.03.84.09 (LMH); the Vietnam Academy of Science and Technology under Grant

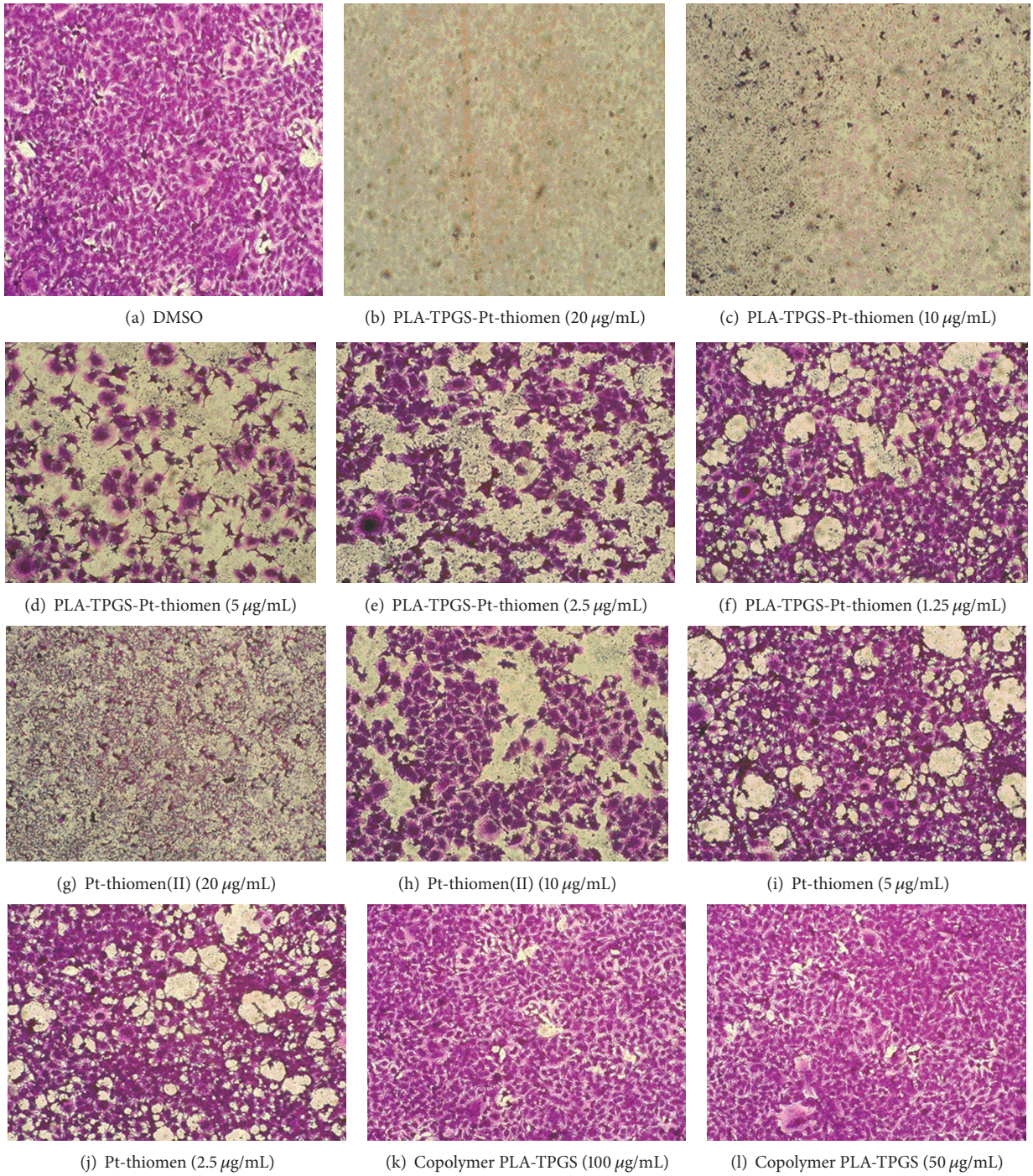

(a) DMSO (b) PLA-TPGS-Pt-thiomen (20 μg/mL) (c) PLA-TPGS-Pt-thiomen (10 μg/mL)

(d) PLA-TPGS-Pt-thiomen (5 μg/mL) (e) PLA-TPGS-Pt-thiomen (2.5 μg/mL) (f) PLA-TPGS-Pt-thiomen (1.25 μg/mL)

(g) Pt-thiomen(II) (20 μg/mL) (h) Pt-thiomen(II) (10 μg/mL) (i) Pt-thiomen (5 μg/mL)

(j) Pt-thiomen (2.5 μg/mL) (k) Copolymer PLA-TPGS (100 μg/mL) (l) Copolymer PLA-TPGS (50 μg/mL)

Figure 7: The images of Hep-G2 cells after 72 h growing in the presence of test samples at different concentrations.

no. VAST03.03/13-14 (HPT), and the Ministry of Science and Technology of Vietnam (MOST) under Bilateral program Vietnam-Germany (2011–2013) 54/2011/HĐ-NĐT (LMH).

References

[1] A. C. Begg, "Cisplatin and radiation: interaction probabilities and therapeutic possibilities," *International Journal of Radiation Oncology Biology Physics*, vol. 19, no. 5, pp. 1183–1189, 1990.

[2] F. M. Muggia, "Recent updates in the clinical use of platinum compounds for the treatment of gynecologic cancers," *Seminars in Oncology*, vol. 31, supplement 14, no. 2, pp. 17–24, 2004.

[3] T. Boulikas and M. Vougiouka, "Cisplatin and platinum drugs at the molecular level," *Oncology Reports*, vol. 10, no. 6, pp. 1663–1682, 2003.

[4] P. Boffetta, A. M. J. Fichtinger-Schepman, E. Weiderpass et al., "Cisplatin-DNA adducts and protein-bound platinum in blood of testicular cancer patients," *Anti-Cancer Drugs*, vol. 9, no. 2, pp. 125–129, 1998.

[5] M. Babincova, V. Altanerova, C. Altaner, C. Bergemann, and P. Babinec, "In vitro analysis of cisplatin functionalized magnetic nanoparticles in combined cancer chemotherapy and electromagnetic hyperthermia," *IEEE Transactions on Nanobioscience*, vol. 7, no. 1, pp. 15–19, 2008.

[6] V. Pinzani, F. Bressolle, I. J. Haug, M. Galtier, J. P. Blayac, and P. Balmes, "Cisplatin-induced renal toxicity and toxicity-modulating strategies: a review," *Cancer Chemotherapy and Pharmacology*, vol. 35, no. 1, pp. 1–9, 1994.

[7] K. Avgoustakis, A. Beletsi, Z. Panagi, P. Klepetsanis, A. G. Karydas, and D. S. Ithakissios, "PLGA-mPEG nanoparticles of cisplatin: in vitro nanoparticle degradation, in vitro drug release and in vivo drug residence in blood properties," *Journal of Controlled Release*, vol. 79, no. 1–3, pp. 123–135, 2002.

[8] V. B. Jadhav, Y. J. Jun, J. H. Song et al., "A novel micelle-encapsulated platinum (II) anticancer agent," *Journal of Control Release*, vol. 147, no. 1, pp. 144–150, 2010.

[9] A. D. Carvalho Jr., F. P. Vieira, V. J. De Melo et al., "Preparation and cytotoxicity of cisplatin-containing liposomes," *Brazilian Journal of Medical and Biological Research*, vol. 40, no. 8, pp. 1149–1157, 2007.

[10] G. P. Stathopoulos, "Liposomal cisplatin: a new cisplatin formulation," *Anti-Cancer Drugs*, vol. 21, no. 8, pp. 732–736, 2010.

[11] L. M. Huong, H. P. Thu, N. T. B. Thuy et al., "Preparation and antitumor-promoting activity of curcumin encapsulated by 1,3-β-glucan isolated from Vietnam medicinal mushroom *Hericium erinaceum*," *Chemistry Letters*, vol. 40, no. 8, pp. 846–848, 2011.

[12] H. P. Thu, D. T. Quang, M. T. T. Trang et al., "*In vitro* apoptosis enhancement of Hep-G2 Cells by PLA-TPGS and PLA-PEG block copolymer encapsulated curcumin nanoparticles," *Chemistry Letters*, vol. 42, no. 3, pp. 255–257, 2013.

[13] S. Dhar, F. X. Gu, R. Langer, O. C. Farokhza, and S. J. Lippard, "Targeted delivery of cisplatin to prostate cancer cells by aptamer functionalized Pt(IV) prodrug-PLGA-PEG nanoparticles," *Proceedings of the National Academy of Sciences of the United States of America*, vol. 105, no. 45, pp. 17356–17361, 2008.

[14] N. Poonia, M. S. Kumar, D. Arora, and N. Mahadevan, "Development of cisplatin loaded poly (d, l-lactide-co-glycolide)-poly (ethylene glycol) immunonanopaticles for epidermal growth factor receptor (EGFR) positive pancreatic cancer cells," *International Journal of Recent Advances in Pharmaceutical Research*, vol. 3, pp. 14–24, 2011.

[15] G. Mattheolabakis, E. Taoufik, S. Haralambous, M. L. Roberts, and K. Avgoustakis, "*In vivo* investigation of tolerance and antitumor activity of cisplatin-loaded PLGA-mPEG nanoparticles," *European Journal of Pharmaceutics and Biopharmaceutics*, vol. 71, no. 2, pp. 190–195, 2009.

[16] H. Xiao, D. Zhou, S. Liu, Y. Zheng, Y. Huang, and X. Jing, "A complex of cyclohexane-1,2-diaminoplatinum with an amphiphilic biodegradable polymer with pendant carboxyl groups," *Acta Biomaterialia*, vol. 8, no. 5, pp. 1859–1868, 2012.

[17] S. Utku, M. Topal, A. Dogen, and M. S. Serin, "Synthesis, characterization, antibacterial and antifungal evaluation of some new platinum(II) complexes of 2-phenylbenzimidazole ligands," *Turkish Journal of Chemistry*, vol. 34, no. 3, pp. 427–436, 2010.

[18] M. Akbar Ali, A. H. Mirza, R. J. Butcher, M. T. H. Tarafder, T. B. Keat, and A. M. Ali, "Biological activity of palladium(II) and platinum(II) complexes of the acetone Schiff bases of S-methyl- and S-benzyldithiocarbazate and the X-ray crystal structure of the [Pd(asme)2] (asme=anionic form of the acetone Schiff base of S-methyldithiocarbazate) complex," *Journal of Inorganic Biochemistry*, vol. 92, no. 3-4, pp. 141–148, 2002.

[19] V. Vichai and K. Kirtikara, "Sulforhodamine B colorimetric assay for cytotoxicity screening," *Nature Protocols*, vol. 1, no. 3, pp. 1112–1116, 2006.

[20] P. Skehan, R. Storeng, D. Scudiero et al., "New colorimetric cytotoxicity assay for anticancer-drug screening," *Journal of the National Cancer Institute*, vol. 82, no. 13, pp. 1107–1112, 1990.

[21] A. K. Mishra and N. K. Kaushik, "Synthesis, characterization, cytotoxicity, antibacterial and antifungal evaluation of some new platinum (IV) and palladium (II) complexes of thiodiamines," *European Journal of Medicinal Chemistry*, vol. 42, no. 10, pp. 1239–1246, 2007.